Phase Morphology Control of Immiscible Polymer Blends under Vibration Force Field

Yao-Xue Du,[1,2] Jin-Ping Qu[1]

[1]*National Engineering Research Center of Novel Equipment for Polymer Processing, South China University of Technology, Guangzhou 510640, China*
[2]*Department of Electromechanical Engineering, Wuyi University, Jiangmen 529020, P. R. China*

Received 27 August 2005; accepted 20 March 2006
DOI 10.1002/app.24445
Published online in Wiley InterScience (www.interscience.wiley.com).

ABSTRACT: The formulas of polymer melt velocity, shearing rate, and shearing stress under vibration force field are established through simplifying coaxial cylinder circular flow into plane motional flow. On the basis of the concept of energy ratio model, the rate of energy dissipation and the energy ratio about blending systems are expressed, and the affected factors on phase morphology are studied theoretically. The calculated and analytical results of dynamic flow field and energy ratio show that with the increasing of vibration strength, the fluctuating shearing force field exerted on polymer melt and the negative pressure diffusion behavior of instantaneous impulse strengthen. The energy consumption for phase inversion of immiscible polymer blends under vibration force field is less than that of steady state. The parameter controllability of vibration force field provides a more effective method for realizing phase inversion of immiscible polymer blends. The analysis of transmission electron microcopy micrographs of ethylene–propylene–diene terpolymer/polypropylene blends verifies that the energy ratio model and its phase morphology controlling theory have a good coincidence in comparison with experimental results. © 2006 Wiley Periodicals, Inc. J Appl Polym Sci 102: 2299–2307, 2006

Key words: immiscible polymer blends; phase morphology; dynamic flow field; vibration force field; energy ratio model

INTRODUCTION

Multiphase polymer morphology depends on blends component, performance, and processing condition. With the increasing dispersed phase concentration, the cocontinuous morphology is formed because of particles coalescence, which results in phase inversion. Willemse et al.[1] thought that the position and range of phase inversion concentration for polymer blends is affected by interfacial tension. With the increasing interfacial tension, the composed range of cocontinuous structure becomes narrow. Interfacial tension also affects morphological stability of cocontinuous structure and phase dimension. Different phase morphology of immiscible polymer blends results in their performance difference. Therefore, establishing phase inversion models of immiscible polymer blends can not only be used to judge phase morphology theoretically, but also obtain final required phase morphology and produce high performance product. At present, mathematical models of phase inversion have viscosity ratio, elasticity ratio, viscoelasticity ratio, and torque ratio models.

Using viscosity ratio model[2–4] can predict that low viscosity component has a trend to form continuous phase only at low shearing rate. With the increasing shearing rate, the concentration error of predicting phase inversion zone is increased in comparison with experimental observation. Therefore, this model has limitation to identify phase inversion of immiscible polymer blends.

Bourry and Favis[5] thought elasticity as important parameter and expressed phase inversion with storage modulus. Elasticity ratio model shows that more elastic phase easily covers less elastic phase to form matrix at high enough concentration. Compared with viscosity ratio model, this model can predict phase inversion more accurately at the range of high concentration and shearing rate.

Viscosity ratio and elasticity ratio models are based on component phase inversion concentration and viscosity or elasticity, whereas polymer blends are viscoelastic fluid at molten state. Vanoene theory[6] showed that the component with larger second normal stress easily forms dispersed phase. Therefore, Tang et al.[7] proposed a phase inversion expression based on blend's viscoelasticity, namely viscoelasticity ratio model. Bourry and Favis[5] thought that the effects of viscosity and elasticity should be considered at studying HDPE/PS blends.

Correspondence to: Y.-X. Du (luoting@wyu.cn).
Contract grant sponsor: Guangdong Natural Science Foundation of China; contract grant number: 04011763.
Contract grant sponsor: Guangdong Science and Technology Program of China; contract grant number: 2005B10201010.

Through experiment Mekhilef and Verhoogt[8] thought that Avgeropoulos model,[3] namely torque ratio model, could predict phase inversion point better than viscosity ratio model. According to the penetration theory, this model can be used at the range of torque ratio 0.18–5.4 theoretically. Ho et al.[9] also discovered the relation between volume fraction and torque ratio.

Because the above models consider the affected factors on phase morphology too simple, they could result in more error when compared with experimental results and cannot predict phase morphology at different materials and processing condition exactly. Thus, the applied field has more limitation. It is the reason that the affected factors on phase morphology of immiscible polymer blends have not only blends component, but also polymer structural parameters and rheological behavior as well as processing condition. Therefore, it is necessary to establish an effective mathematical model of judging phase inversion, in which the finally desired phase morphology can be controlled through considering the dependence of blends phase morphology on material property and processing condition.

DYNAMIC FLOW FIELD

Polymer electromagnetic dynamic processing technique[10] is an important innovation in the field of polymer processing. The key of this technique is that vibration force field is introduced to polymer processing, which makes traditional polymer processing mechanism to change and many new phenomena, which do not possess in traditional processing, appeared. Under vibration force field, processing temperature, viscosity and elasticity of polymer melt decrease, plasticizing and mixing effects, product quality, and joint situation of two-phase interface become better. The experimental research shows that vibration force field can make agglomerating $CaCO_3$ particles with high surface energy easily fracture and homogeneously disperse in matrix.[11] Moreover, because extrusion swelling of polymer melt becomes smaller, the disadvantageous influence on dimensional accuracy and appearance quality of product reduces, which benefits to realize stable extrusion and improve product quality.

To study the performance and phase morphology of immiscible polymer blends as well as the intensifying effect of vibration force field, a miniature vibration mixing equipment is designed. Processed material moves in the circular gap composed of inner and outer cylinders, which produces rotating Couette flow. When polymer melt moves in the circular gap, outer cylinder is the barrel and keeps at rest, and inner cylinder produces axial reciprocal vibration exerted by a vibration unit besides circular rotation. Because the circular gap height between coaxial cylinders is much less than cylindrical radius, the influence of cylindrical curvature can be ignored. The approximate hypothesis of plane motion is made, and the physical model is shown in Figure 1. According to relative motion principle, hypothesizing that inner cylinder (static plate) relatively rests, then outer cylinder (moving plate) produces axial reciprocal vibration at the time of circular rotation. In Figure 1, v_0 is circular velocity of moving plate in direction x, $v_0A_a \cos \omega t$ is axial vibration velocity of moving plate in direction z, and H is circular gap height. If hypothesizing polymer melt as non-Newtonian fluid with isothermal incompressible streamlined flow and no wall slippage, and neglecting the influence of body force, then momentum equation of polymer melt between two plates is:

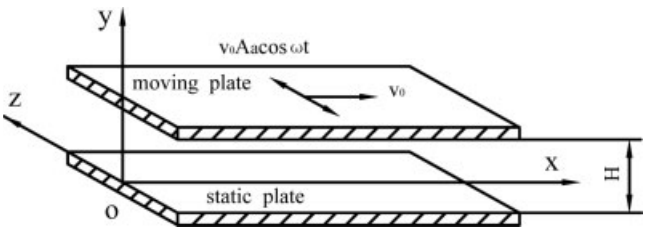

Figure 1 Plane motional flow.

$$\begin{cases} \rho \dfrac{\partial v_x}{\partial t} = -\dfrac{\partial p}{\partial x} + \dfrac{\partial \tau_{yx}}{\partial y} \\ \rho \dfrac{\partial v_z}{\partial t} = -\dfrac{\partial P}{\partial z} + \dfrac{\partial \tau_{yz}}{\partial y} \end{cases}$$

where ρ is density, v_x is velocity of direction x, v_z is velocity of direction z, t is time, p is pressure, τ_{yx} and τ_{yz} are shearing stresses. Because polymer melt is only acted by drag flow and is not acted by pressure flow in the circular gap, the influence of pressure gradient is not considered. Moreover, inertial item is also ignored at considering velocity static solution. Thus, the above equation can be simplified:

$$\begin{cases} \dfrac{\partial \tau_{yx}}{\partial y} = 0 \\ \dfrac{\partial \tau_{yz}}{\partial y} = 0 \end{cases} \tag{1}$$

The constitutive equation that reflects material parameters must be established when solving momentum equation. Owing to introduction of vibration force field, melt flow becomes unsteady, and polymer elastic response becomes more important. In Maxwell linear viscoelastic constitutive equation, viscosity can be expressed with depending on shearing rate, and relaxation time is hypothesized independent of shearing rate. Thus, Tanner constitutive equation[12] can be obtained:

$$\vec{\tau} + \lambda \frac{\partial \vec{\tau}}{\partial t} = \eta\left(\dot{\vec{\gamma}}\right)\dot{\vec{\gamma}} \tag{2}$$

where $\vec{\tau}$ is partial stress tensor, λ is melt relaxation time, and $\dot{\vec{\gamma}}$ is deformation rate tensor.

Revising eq. (2), namely expressing $\eta\left(\vec{\dot{\gamma}}\right)$ with:

$$\eta(\vec{\dot{\gamma}}) = K\left(\frac{1}{2}II_{\Delta}\right)^{(n-1)/2}$$

where K is consistency coefficient and n is flow index. Whereas $\frac{1}{2}II_{\Delta}$ is second invariant of deformation rate tensor, and can be expressed with:

$$\frac{1}{2}II_{\Delta} = \left(\frac{\partial v_x}{\partial y}\right)^2 + \left(\frac{\partial v_z}{\partial y}\right)^2 \approx \left(\frac{v_0}{H}\right)^2 + \left(\frac{v_0 A_a \cos\omega t}{H}\right)^2 = \left(\frac{v_0}{H}\right)^2 (1 + A_a^2 \cos^2\omega t)$$

Giving $\eta_0 = K\left(\frac{v_0}{H}\right)^{n-1}$ is melt nominal apparent viscosity of pure shearing flow at v_0, then:

$$\eta(\vec{\dot{\gamma}}) = \eta_0(1 + A_a^2 \cos^2\omega t)^{(n-1)/2}$$

Thus, revised Tanner constitutive equation can be further expressed with component form:

$$\begin{cases} \tau_{yx} + \lambda\dfrac{\partial \tau_{yx}}{\partial t} = \eta_0(1 + A_a^2\ \cos^2\omega t)^{\frac{n-1}{2}}\dfrac{\partial v_x}{\partial y} \\ \tau_{yz} + \lambda\dfrac{\partial \tau_{yz}}{\partial t} = \eta_0(1 + A_a^2\ \cos^2\omega t)^{\frac{n-1}{2}}\dfrac{\partial v_z}{\partial y} \end{cases} \tag{3}$$

Hypothesize that axial vibration displacement of moving plate is:

$$S = S_0\ \sin\omega t$$

then axial velocity variation of moving plate is:

$$v_z^*(t) = \frac{dS}{dt} = S_0\omega\ \cos\omega t$$

where S_0 is axial vibration amplitude and ω is axial vibration circular frequency. Giving $A_a = \frac{S_0\omega}{v_0}$ is axial vibration strength coefficient, then the above equation can be written:

$$v_z^*(t) = v_0 A_a\ \cos\omega t$$

Thus, the velocity boundary conditions can be obtained:

$$\begin{cases} v_x|_{y=0} = 0 \\ v_z|_{y=0} = 0 \end{cases} \text{ and } \begin{cases} v_x|_{y=H} = v_0 \\ v_z|_{y=H} = v_0 A_a\ \cos\omega t \end{cases} \tag{4}$$

Deriving eq. (3) to y, using momentum eq. (1) and boundary conditions eq. (4), melt velocity of directions x and z can be expressed with:

$$\begin{cases} v_x = \dfrac{v_0}{H}y \\ v_z = \dfrac{v_0 A_a \cos\omega t}{H}y \end{cases} \tag{5}$$

and melt shearing rate can be expressed with:

$$\begin{cases} \dot{\gamma}_{yx} = \dfrac{\partial v_x}{\partial y} = \dfrac{v_0}{H} \\ \dot{\vec{\gamma}}_{yz} = \dfrac{\partial v_z}{\partial y} = \dfrac{v_0 A_a \cos\omega t}{H} \end{cases} \tag{6}$$

Introducing eq. (6) to eq. (3) and solving it, shearing stress can be obtained:

$$\begin{cases} \tau_{yx} = e^{t/\lambda}\left[\dfrac{\eta_0 v_0}{\lambda H}\displaystyle\int(1 + A_a^2\cos^2\omega t)^{(n-1)/2}e^{t/\lambda}dt + C_1\right] \\ \tau_{yz} = e^{t/\lambda}\left[\dfrac{\eta_0 v_0}{\lambda H}\displaystyle\int A_a\cos\omega t(1 + A_a^2\cos^2\omega t)^{(n-1)/2}e^{t/\lambda}dt + C_2\right] \end{cases}$$

Utilizing binomial formula and considering $A_a << 1$, then ignoring more than quadratic of A_a, and only considering steady state of fluctuating shearing stress, namely the state at $t \to \infty$, shearing stress can be further expressed with:

$$\begin{cases} \tau_{yx} = \dfrac{\eta_0 v_0}{H} + \dfrac{\eta_0 v_0 (n-1)A_a^2}{4H}\left[1 + \dfrac{\cos(2\omega t - \phi_2)}{\sqrt{1 + 4\lambda^2\omega^2}}\right] \\ \tau_{yz} = \dfrac{\eta_0 v_0 A_a}{H\sqrt{1 + \lambda^2\omega^2}}\cos(\omega t - \phi_1) \end{cases} \tag{7}$$

Giving $\overline{v}_x = \frac{v_x}{v_0}$, $\overline{v}_z = \frac{v_z}{v_0}$, $\overline{y} = \frac{y}{H}$, $\overline{t} = \frac{t}{T_0}$, whereas $T_0 = \frac{2\pi}{\omega}$, making eq. (5) dimensionless and omitting top line, then dimensionless velocity can be obtained:

$$\begin{cases} v_x = y \\ v_z = A_a\ y\cos 2\pi t \end{cases} \tag{8}$$

Giving $\overline{\dot{\gamma}}_{yx} = \frac{\dot{\gamma}_{yx}H}{v_0}$ and $\overline{\dot{\gamma}}_{yz} = \frac{\dot{\gamma}_{yz}H}{v_0}$, making eq. (6) dimensionless and omitting top line, then dimensionless shearing rate can be obtained:

$$\begin{cases} \dot{\gamma}_{yx} = 1 \\ \dot{\gamma}_{yz} = A_a\ \cos 2\pi t \end{cases} \tag{9}$$

Giving $\overline{\tau}_{yx} = \frac{\tau_{yx}H}{\eta_0 v_0}$, $\overline{\tau}_{yz} = \frac{\tau_{yz}H}{\eta_0 v_0}$ and $\tau_0 = \frac{\lambda}{T_0}$, whereas $\phi_1 = arctg2\pi\tau_0$, $\phi_2 = arctg4\pi\tau_0$, making eq. (7) dimensionless and omitting top line, then dimensionless shearing stress can be obtained:

$$\begin{cases} \tau_{yx} = 1 + \dfrac{(n-1)A_a^2}{4}\left[1 + \dfrac{\cos(4\pi t - \phi_2)}{\sqrt{1 + 16\pi^2\tau_0^2}}\right] \\ \tau_{yz} = \dfrac{A_a}{\sqrt{1 + 4\pi^2\tau_0^2}}\cos(2\pi t - \phi_1) \end{cases} \tag{10}$$

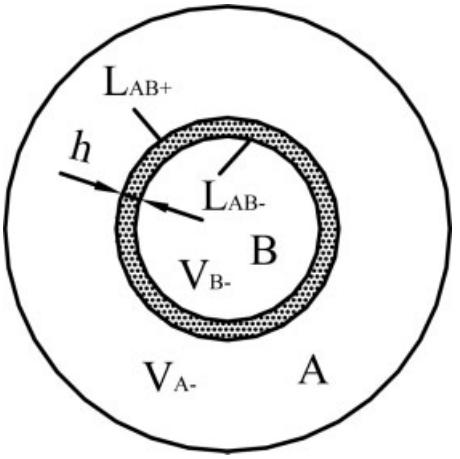

Figure 2 Controlling volume model.

PHASE MORPHOLOGY CONTROL

Concept of energy ratio model

System inner energy is changed during polymer blending, which makes blending systems unstable and phase morphology varied, and is related to system energy input from the outer. Whereas the amount of energy is related to shearing stress, blends viscosity, and elasticity, and is affected by blends component and property as well as processing condition. Thus, it is one of the best methods to study phase morphology of immiscible polymer blends from the view of energy.

Phase morphology of immiscible polymer blends at dynamic stable equilibrium can be only phase morphology I (component A as continuous phase, component B as dispersed phase) or phase morphology II (component B as continuous phase, component A as dispersed phase) under certain condition. According to material energetic principle, blending systems always keep minimum energy state. Through calculating and comparing the rates of energy dissipation between phase morphologies I and II, the smaller is final phase morphology at dynamic stable equilibrium. On the basis of the energy concept, the energy ratio model of immiscible polymer blends can be established by defining the ratio of the rates of energy dissipation between phase morphologies I and II as energy ratio E. When $E < 1$, component A is continuous phase and component B is dispersed phase. When $E > 1$, component B is continuous phase and component A is dispersed phase. When $E = 1$, blending systems are cocontinuous morphologic structure.

Mathematical model of phase morphology control

When establishing the mathematical model of phase morphology control, plane motional flow is used to simplify three dimensional flow. Hypothesize that dispersed phase is spherical particle and is distributed homogeneously in continuous phase, and there is no influence on each other. Therefore, multi-particle dispersed blending systems are simplified as single-particle dispersed particles, namely abstracted as single cell model,[13] shown in Figure 2. The boundary conditions of velocity and stress in two-phase interface L_{AB} of controlling volume V are:

$$\begin{cases} (v_A)_t = (v_B)_t \\ (v_A)_n = (v_B)_n \end{cases} \quad \text{and} \quad \begin{cases} (S_A)_{nt} = (S_B)_{nt} \\ (S_A)_{nn} = (S_B)_{nn} = \sigma_{in} H_{in} \end{cases}$$

where v_A and v_B are velocities of phase A and phase B, $(S_A)_{ij}$ and $(S_B)_{ij}$ are the ijth component (with $i = n, t$; $j = n, t$) of stress tensors $\vec{S}_A$ and $\vec{S}_B$ of phase A and phase B, subscripts n and t are normal and tangential directions, σ_{in} is interfacial tension, and H_{in} is interfacial average curvature.

Energy dissipation per unit volume in every controlling volume can be expressed with:

$$\delta\dot{E} = \vec{S} : \vec{\dot{\gamma}} = \sum_i \sum_j S_{ij}\dot{\gamma}_{ji} \tag{11}$$

Expressing stress tensor:

$$\vec{S} = -p\vec{\delta} + \vec{\tau}$$

and deformation rate tensor:

$$\vec{\dot{\gamma}} = \frac{1}{2}\left[\nabla\vec{v} + (\nabla\vec{v})^{\mathrm{T}}\right]$$

with component form, introducing to eq. (11), where $\vec{\delta}$ is unit tensor and $\nabla\vec{v}$ is velocity gradient, noticing that polymer melt flows in the circular gap composed of inner and outer cylinders, then energy dissipation per unit volume in every controlling volume can be further expressed with:

$$\delta\dot{E} = \tau_{yx}\dot{\gamma}_{yx} + \tau_{yz}\dot{\gamma}_{yz} \tag{12}$$

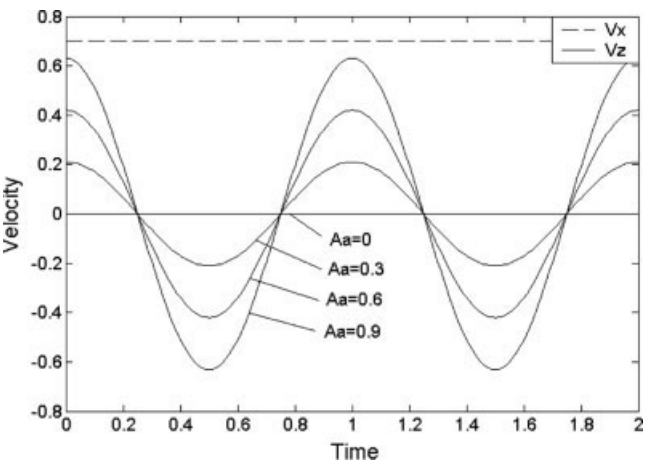

Figure 3 Variation of velocity at different A_a.

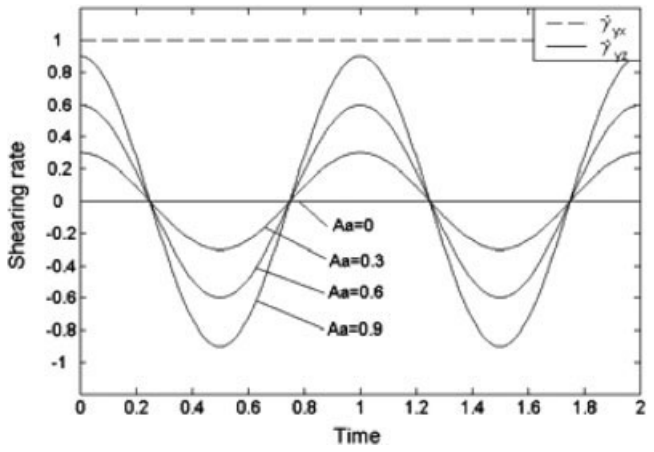

Figure 4 Variation of shearing rate at different A_a.

The rate of energy dissipation in controlling volume can be written as follows:

$$\dot{E} = \int_V \delta\dot{E} dV$$

Controlling volume can be divided into three regions composed of phase A, phase B, and two-phase interface. When interfacial thickness is very thin, the above equation can be rewritten as:

$$\dot{E} = \iint_{V_A} \delta\dot{E} dV + \iint_{V_B} \delta\dot{E} dV + \iint_{V_{AB}} \delta\dot{E} dV \qquad (13)$$

Because the rate of energy dissipation in two-phase interface of controlling volume is equal to the work done by traction force $\vec{F}_i = \boldsymbol{S}_i \cdot \vec{n}$ (with i = A, B, where $\vec{n}$ is unit outward normal vector) along the boundary, the third item in the right of eq. (13) can be expressed with:

$$\iint_{V_{AB}} \delta\dot{E} dV = \left[\int_{L_{AB}} \vec{F}_A \cdot \vec{v} dL + \int_{L_{AB}} \vec{F}_B \cdot \vec{v} dL\right]_{xy} + \left[\int_{L_{AB}} \vec{F}_A \cdot \vec{v} dL + \int_{L_{AB}} \vec{F}_B \cdot \vec{v} dL\right]_{zy}$$

Therefore, utilizing the boundary conditions of velocity and stress in two-phase interface of blending systems, the above equation can be further expressed with:

$$\iint_{V_{AB}} \delta\dot{E} dV = \int_{L_{AB}} \sigma_{in} H_{in} v_{nxy} dL + \int_{L_{AB}} \sigma_{in} H_{in} v_{nzy} dL \qquad (14)$$

where v_{nxy} and v_{nzy} are interface normal velocities in planes xy and zy of controlling volume.

Rate of energy dissipation and energy ratio

The above approximate hypothesis of plane motion is also adopted in studying dispersed phase micro-flow field of coaxial cylinder circular flow under vibration force field, and the physical model is the same as Figure 1. Hypothesize that velocity in two-phase interface is equal, distribution of shearing rate in dispersed phase micro-flow field is concentric circle, and its size is equal at the same direction. Thus, adopting same method, the mathematical model of polymer melt micro-flow field can be obtained. The expressions of shearing rate and shearing stress are the same as polymer melt flow field, but should add the dispersed phase subscript of blending systems.

In the condition of ignoring interfacial thickness, interfacial average curvature between continuous phase A and dispersed phase B is:

$$H_{in} = \frac{2}{R_B} \qquad (15)$$

Melt velocities of continuous phase A and dispersed phase B are same in two-phase interface, and their normal components can be written in polar coordinate form:

$$\begin{cases} v_{nxy} = \dfrac{v_0}{H}(y_0 + R_B \sin\theta)\cos\theta \\ v_{nzy} = \dfrac{v_0 A_a \cos\omega t}{H}(y_0 + R_B \sin\gamma)\cos\gamma \end{cases} \qquad (16)$$

where y_0 is coordinate y of central position in controlling volume, θ and γ are directional angles.

To phase morphology I, utilizing eqs. (12) and (14), introducing eqs. (6) and (7) and eqs. (15) and (16) to eq. (13), then making dimensionless and omitting dimensionless notation, the rate of energy dissipation in controlling volume can be written in dimensionless form:

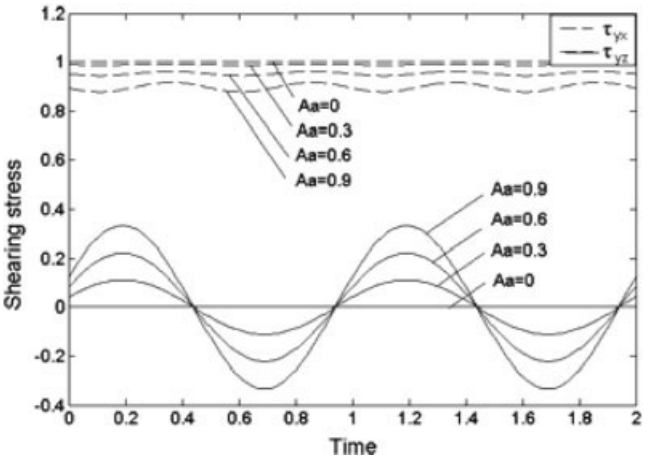

Figure 5 Variation of shearing stress at different A_a.

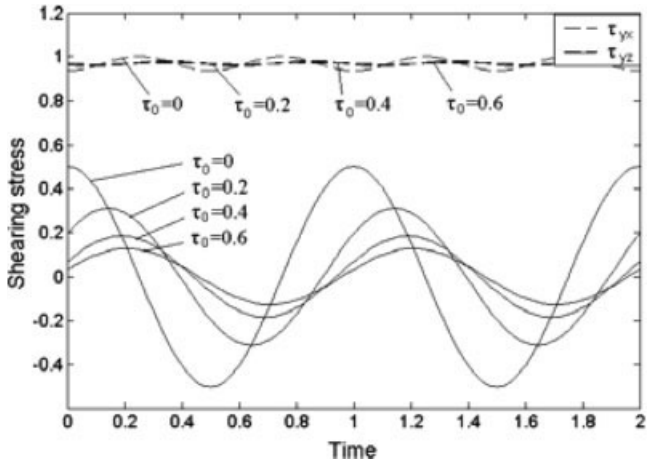

Figure 6 Variation of shearing stress at different τ_0.

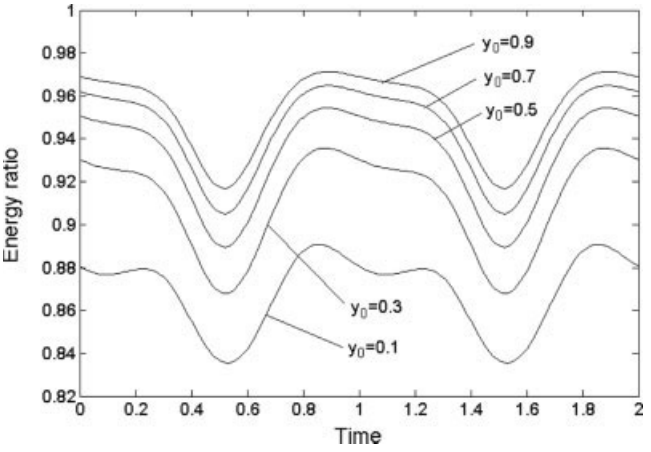

Figure 7 Variation of energy ratio at different y_0.

$$\overline{\dot{E}}_I = d_A(1-\phi_B^{2/3}) + d_B\, p_{\mathrm{BA}}\phi_B^{2/3} + \frac{8y_0\sigma_{\mathrm{in}}\phi_B^{2/3}}{R_{\mathrm{BI}}^2}(1 + A_a\ \cos 2\pi t) \quad (17)$$

where

$$d_i = 1 + \frac{(n_i-1)A_a^2}{4} + \frac{A_a^2}{\sqrt{1+4\pi^2\tau_{i0}^2}}\cos 2\pi t\ \cos(2\pi t - \phi_{i1}) + \frac{(n_i-1)A_a^2}{4\sqrt{1+16\pi^2\tau_{i0}^2}}\cos(4\pi t - \phi_{i2})$$

(with $i = \mathrm{A}, \mathrm{B}$).

In the same manner to phase morphology II, the rate of energy dissipation in controlling volume can be obtained in dimensionless form:

$$\overline{\dot{E}}_{\mathrm{II}} = d_B(1-\phi_A^{2/3}) + \frac{d_A\phi_A^{2/3}}{p_{\mathrm{BA}}} + \frac{8y_0\sigma_{\mathrm{in}}\phi_A^{2/3}}{p_{\mathrm{BA}}R_{\mathrm{AII}}^2}(1 + A_a\ \cos 2\pi t) \quad (18)$$

Therefore, based on the energy ratio model, the expression of judging phase morphology of immiscible polymer blends is

$$E = \frac{1}{p_{\mathrm{BA}}}\left(\frac{R_{\mathrm{BI}}}{R_{\mathrm{AII}}}\right)^2\left(\frac{\phi_A}{\phi_B}\right)^{2/3}\frac{\overline{\dot{E}}_{\mathrm{I}}}{\overline{\dot{E}}_{\mathrm{II}}} \quad (19)$$

where p_{BA} is nominal apparent viscosity ratio of components B and A, ϕ_A and R_{AII} are volume fraction of component a and its dispersed phase radius, ϕ_B and R_{BI} are volume fraction of component B and its dispersed phase radius.

RESULTS AND DISCUSSION

Through the calculation of dynamic flow field in coaxial cylinder circular flow from eq. (8) to eq. (10), the variations of polymer melt velocity, shearing rate, and shearing stress with time under vibration force field are obtained. Figures 3–5 are the calculated results of different vibration strength coefficients. As can be observed in Figure 3, circular velocity of direction x is not affected by vibration force field, whereas axial velocity of direction z is changed with time periodically under axial vibration force field exerted by a vibration unit, and with the increasing of vibration strength coefficient, the axial velocity amplitude of direction z increases.

The velocity fluctuation causes the variation of shearing rate, shown in Figure 4, which is of same changing pattern in directions x and z. Because of the introduction of axial vibration force field, shearing stress is changed periodically not only in directions z but also in directions x, shown in Figure 5. Because polymer melt

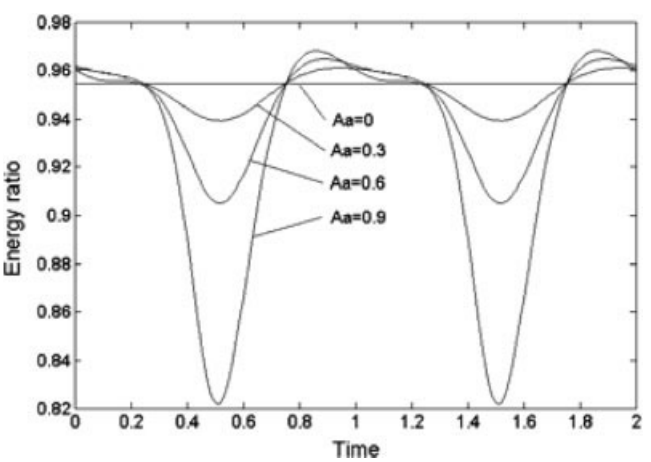

Figure 8 Variation of energy ratio at different A_a.

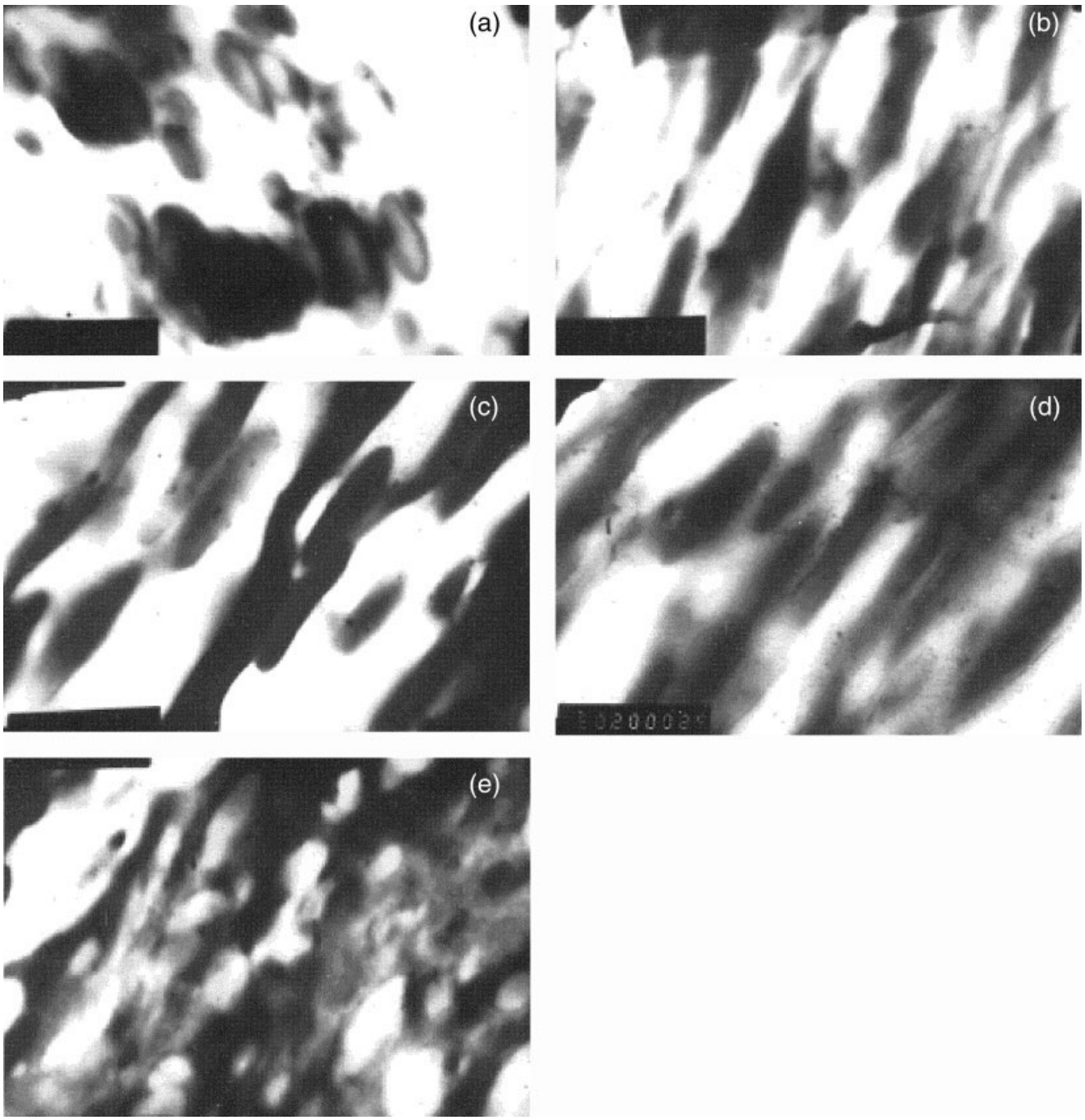

Figure 9 TEM micrographs of EPDM/PP blends with blend ratio of (a) 20/80, (b) 40/60, (c) 50/50, (d) 60/40, and (e) 80/20.

is acted by fluctuating shearing force field, macromolecular chains obtain instantaneous impulse, and local negative pressure space is produced in the vicinity of segment, which strengthens segmental diffusion and motion by pressure difference. With the increasing vibration strength, the pulsating amplitude of shearing stress increases, and instantaneous impulse and local negative pressure space of macromolecular chain and segment increase further. Thus, entanglement and inner frictional force of macromolecular chain and segment reduce, which makes macromolecular chain creep more quickly. Polymer melt becomes thin, apparent viscosity lowers, flowing resistance reduces, and diffusion and motion of macromolecular chain strengthen. As can be observed in Figure 4, even though periodical vibration is exerted only in axial direction, polymer melt can be also acted by periodical shearing stress in circular direction, which is characteristic of viscoelastic response behavior in polymer melt. It shows that introducing vibration force field to polymer processing can induce chaos mixing, enhance plasticizing and mixing effects, realize low temperature

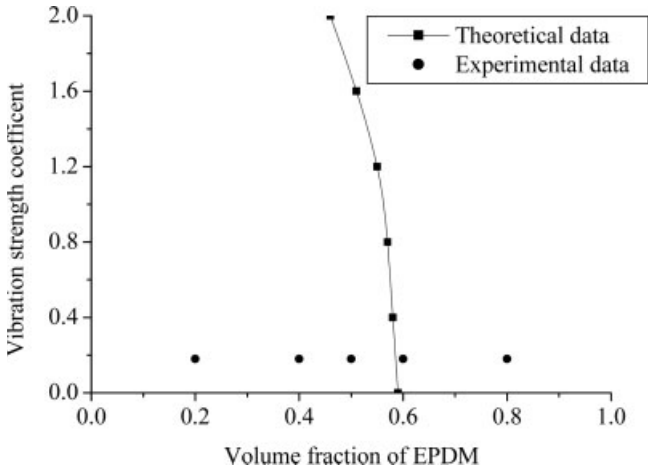

Figure 10 Comparison of phase morphology between theory and experiment.

processing, reduce energy consumption, and improve product properties.

Figure 6 is the variation of shearing stress with time at different relaxation time. It shows that shearing stress is changed periodically with time in axial and circular directions, but the strength amplitude of circular pulsation is not as prominent as that of axial pulsation, because the direction of vibration force field is along axial action. Whether shearing stress is in circular or axial directions, the phase difference exists between shearing stress and vibration source, and the lag phenomenon is produced. With increasing relaxation time, the pulsating amplitude of shearing force field gradually decreases, the phase angle increases, and the influence of elastic behavior on polymer melt strengthens.

Figures 7 and 8 are the variation of energy ratio with time under certain condition. Figure 7 is the size of energy ratio at different position of flow field, which shows that energy ratio is changed periodically under vibration force field. Owing to the difference of flow field strength at different position, the size of energy ratio is different. Because energy ratio is always less than one, immiscible polymer blends are of phase morphology I, namely component A as continuous phase and component B as dispersed phase.

Figure 8 is the influence of different vibration strength coefficients on energy ratio, which shows that energy ratio keeps constant at steady state and is changed with time periodically after exerting vibration force field. Because the minimum energy ratio at dynamic state in one period is less than that at steady state and with the increasing vibration strength coefficient, the minimum energy ratio decreases, the average value of dynamic energy ratio in one cycle reduces. It shows that vibration force field can effectively control phase morphology of immiscible polymer blends, and energy consumption for realizing phase inversion of blending systems is less than that at steady state. The reason is the instantaneous impulse effect produced by vibration force field, which makes polymer melt processing temperature lower as well as viscosity and elasticity reduce. Therefore, entanglement density of polymer melt decreases, agglomerating dispersed phase particles with high surface energy are easily fractured and homogeneously dispersed in matrix, which can shorten the required time of phase inversion and reduce energy consumption during processing. In addition, the analysis of applying energy ratio model to phase morphology of immiscible polymer blends shows that whether steady state or dynamic state, blending systems are of phase morphology I because energy ratio is always less than one. With the increasing vibration strength, the stable margin that blending systems keep phase morphology I increases, and the stability improves.

Micrographs of ethylene–propylene–diene terpolymer and polypropylene (EPDM/PP) blends with blend ratio expressed by weight at dynamic processing condition, illustrated in Figure 9, in which the dark areas represent EPDM and the white areas represent PP, are taken using transmission electron microcopy (TEM) to verify the theoretical correctness. When using TEM, the specimens are microtomed into very thin slices and stained with osmium tetroxide (OsO_4) to increase the contrast between rubber and plastic phases. It is apparent that for the EPDM/PP ratios of 20/80, 40/60, and 50/50, EPDM forms dispersed phase, and PP forms continuous matrix. However, at the ratios of 60/40 and 80/20, EPDM becomes continuous matrix, and PP becomes dispersed phase. Therefore, phase inversion occurs between the ratios of 50/50 and 60/40.

The theoretical and experimental results of EPDM/PP blends phase morphology at different volume fraction of EPDM and vibration strength coefficient are showed in Figure 10. The theoretical curve, namely the critical curve of occurring phase inversion, which is got through introducing eqs. (17) and (18) to eq. (19), illustrates that rubber and plastic phases become cocontinuous morphological structure. The curve left region shows EPDM as dispersed phase and PP as continuous matrix, and the curve right region shows EPDM as continuous matrix and PP as dispersed phase. The solid dot, which is obtained from Figure 9, denotes the experimental observed results at vibration strength coefficient of 0.18. Figure 10 shows that the theoretical curve of expressing phase morphology of immiscible polymer blends has a good coincidence in comparison with the experimental results, because phase morphology of EPDM being dispersed phase and PP being continuous matrix is just in the left side of the curve, and the right side of the curve also has the same results as TEM micrographs of EPDM/PP blends. EPDM becomes dispersed phase even though EPDM/PP is 50/50 because of its high viscosity. But, with the increasing EPDM content, EPDM has a tendency of forming continuous matrix. When EPDM/PP is 60/40, EPDM fully becomes

continuous matrix. Therefore, theoretical phase inversion point takes place at a blend ratio of EPDM/PP between 50/50 and 60/40, and critical volume fraction of EPDM is about 0.58, which verifies that the energy ratio model and its phase morphology controlling theory are correct.

CONCLUSIONS

1. With the increasing vibration strength, amplitudes of melt velocity, shearing rate, and shearing stress along the direction of vibration force field in flow field increase, action of fluctuating shearing force field and diffusive behavior of instantaneous impulse negative pressure strengthen. Introduction of vibration force field affects macromolecular motion state, aggregation structure, and rheological behavior, and induces chaos mixing, which can enhance plasticizing and mixing effects, reduce energy consumption, and improve product properties.
2. The phase difference is existed between shearing force field and vibration source. With the increasing relaxation time of polymer melt, the phase angle increases, the pulsating amplitude of shearing force field reduces, lag phenomenon becomes obvious, and the elastic behavior of polymer melt strengthens.
3. The difference of flow field strength at different position makes the size of energy ratio different. Energy consumption for realizing phase inversion of immiscible polymer blends under vibration force field is less than that of steady state.
4. Based on the concept of energy ratio model, the influence of blends component, material rheological behavior, phase dimension, flow field strength, processing condition, and vibration strength on phase inversion of blending systems can be considered overall. Especially, the parameters of vibration force field are easily controlled, which plays an active role in deciding phase inversion factors and provides a more effective method for realizing phase inversion of immiscible polymer blends. The analysis of TEM micrographs of EPDM/PP blends verifies that the energy ratio model and its phase morphology controlling theory have a good coincidence in comparison with experimental results.

References

1. Willemse, R. C.; Posthuma de Boer, A.; van Dam, J.; Gotsis, A. D. Polymer 1999, 40, 827.
2. Jordhamo, G. M.; Manson, J. A.; Sperling, L. H. Polym Eng Sci 1986, 26, 517.
3. Avgeropoulos, G. N.; Weissert, F. C.; Böhm, G. A. Rubber Chem Technol 1976, 49, 93.
4. Miles, I. S.; Zurek, A. Polym Eng Sci 1988, 28, 796.
5. Bourry, D.; Favis, B. D. J Polym Sci Part B: Polym Phys 1998, 36, 1889.
6. Vanoene, H. J Colloid Interface Sci 1972, 40, 448.
7. Tang, T.; Chen, H.; Huang, B. T. Polym Mater Sci Eng 1995, 11, 60.
8. Mekhilef, N.; Verhoogt, H. Polymer 1996, 37, 4069.
9. Ho, R. M.; Wu, C. H.; Su, A. C. Polym Eng Sci 1990, 30, 511.
10. Qu, J. P. China Plast 1997, 11, 69.
11. Qu, J. P.; Wu, Q. B.; Peng, X. F. Eng Plast Appl 2000, 28, 10.
12. Qu, J. P.; Feng, Y. H.; Ren, H. L. China Plast Ind 2001, 29, 28.
13. Han, C. D.; Sun, J.; Chuang, H. K.; Lee, J. K. Polym Eng Sci 1998, 38, 1154.